

Japanese VLBI Network Observations of Radio-Loud Narrow-Line Seyfert 1 Galaxies

Akihiro DOI,^{1,2} Kenta FUJISAWA,¹ Makoto INOUE,³ Kiyooki WAJIMA,^{4,1} Hiroshi NAGAI,^{5,3}
Keiichiro HARADA,¹ Kousuke SUEMATSU,¹ Asao HABE,⁶ Mareki HONMA,^{3,5}
Noriyuki KAWAGUCHI,^{3,5} Eiji KAWAI,⁷ Hideyuki KOBAYASHI,^{8,3} Yasuhiro KOYAMA,⁷
Hiromitsu KUBOKI,⁷ Yasuhiro MURATA,^{2,9} Toshihiro OMODAKA,¹⁰ Kazuo SORAI,⁶
Hiroshi SUDOU,¹¹ Hiroshi TAKABA,¹¹ Kazuhiro TAKASHIMA,¹²
Koji TAKEDA,¹⁰ Sayaka TAMURA,^{9,2} and Ken-ichi WAKAMATSU¹¹

¹*Faculty of Science, Yamaguchi University, 1677-1 Yoshida, Yamaguchi, Yamaguchi 753-8512*

²*The Institute of Space and Astronautical Science, Japan Aerospace Exploration Agency,
3-1-1 Yoshinodai, Sagamihara, Kanagawa 229-8510*

³*National Astronomical Observatory of Japan, 2-21-1 Osawa, Mitaka, Tokyo 181-8588*

⁴*Korea Astronomy and Space Science Institute, 61-1 Whaam-dong, Yuseong, Daejeon 305-348, Korea*

⁵*Department of Astronomical Science, The Graduate University for Advanced Studies (SOKENDAI),
2-21-1 Osawa, Mitaka, Tokyo 181-8588*

⁶*Division of Physics, Graduate School of Science, Hokkaido University, N10W8, Sapporo 060-0810*

⁷*Kashima Space Research Center, National Institute of Information and Communications Technology,
893-1 Hirai, Kashima, Ibaraki 314-8510*

⁸*Mizusawa VERA Observatory, 2-12 Hoshigaoka, Mizusawa, Oshu, Iwate 023-0861*

⁹*Department of Space and Astronautical Science, The Graduate University for Advanced Studies (SOKENDAI),
3-1-1 Yoshinodai, Sagamihara, Kanagawa 229-8501*

¹⁰*Faculty of Science, Kagoshima University, 1-21-30 Korimoto, Kagoshima, Kagoshima 890-0065*

¹¹*Faculty of Engineering, Gifu University, 1-1 Yanagido, Gifu 501-1193*

¹²*Geographical Survey Institute, 1 Kitasato, Tsukuba, Ibaraki 305-0811*

(Received 2006 August 31; accepted 2007 April 9)

Abstract

We performed phase-reference very long baseline interferometry (VLBI) observations on five radio-loud narrow-line Seyfert 1 galaxies (NLS1s) at 8.4 GHz with the Japanese VLBI Network. Each of the five targets (RXS J08066+7248, RXS J16290+4007, RXS J16333+4718, RXS J16446+2619, and B3 1702+457) in milli-Jansky levels were detected and unresolved in milli-arcsecond resolutions, i.e., with brightness temperatures higher than 10^7 K. The nonthermal processes of active galactic nucleus activity, rather than starbursts, are predominantly responsible for the radio emissions from these NLS1s. Out of the nine known radio-loud NLS1s, including those chosen for this study, we found that the four most radio-loud objects exclusively have inverted spectra. This suggests a possibility that these NLS1s are radio-loud due to Doppler beaming, which can apparently enhance both the radio power and the spectral frequency.

Key words: galaxies: active — galaxies: jets — galaxies: Seyfert — radio continuum: galaxies — techniques: interferometric

1. Introduction

Narrow-line Seyfert 1 galaxies (NLS1s), a class of active galactic nuclei (AGNs), are defined as having the following optical properties: (1) the full-width at half-maximum (FWHM) of H β is less than 2000 km s^{-1} , (2) permitted lines are only slightly broader than the forbidden lines, and (3) $[\text{O III}]/\text{H}\beta < 3$ (Osterbrock & Pogge 1985; Pogge 2000). NLS1s have been extensively studied in both optical and X-ray bands; results show that many of their properties are clearly different from those of the classical Seyfert galaxies. There is increasing evidence that NLS1s are extreme AGNs, with accretion rates near to the Eddington limit (e.g., Pounds et al. 1995; Boroson 2002) onto relatively lower mass ($\sim 10^6 M_{\odot}$) black holes (Peterson et al. 2000; Grupe & Mathur

2004), although this picture is still under debate. On the other hand, the radio properties of NLS1s have not been well investigated; to date, there are only two known systematic surveys (Ulvestad et al. 1995; Moran 2000). From these two surveys, unlike the optical and X-ray studies, the radio data showed little difference between NLS1s and classical Seyfert galaxies. Zhou and Wang (2002) suggested that there is a scarcity of radio-loud NLS1s, particularly very radio-loud ones (see also Komossa et al. 2006a). Radio loudness, R , was conventionally defined as the ratio of 5-GHz radio to B -band flux densities, with a threshold of $R = 10$ separating radio-loud and radio-quiet objects (e.g., Visnovsky et al. 1992; Stocke et al. 1992; Kellermann et al. 1994). The reason for the scarcity of radio-loud ($R > 10$) NLS1s is still unknown. The radio-quietness of NLS1s may possibly be related to

the suppression of radio jets emanated from accretion disks with high accretion rates (Greene et al. 2006), as well as X-ray binaries in the *high/soft* state (see, e.g., McClintock & Remillard 2003 for a review).

Radio-loud ($R > 10$) NLS1s are rare, but they do exist (Siebert et al. 1999; Grupe et al. 2000; Zhou et al. 2003; Whalen et al. 2006; Komossa et al. 2006a, 2006b). One possible idea that could explain the existence of radio-loud NLS1s is that nonthermal jets are associated with NLS1s, and a relativistic effect on these jets influences the radio loudness of NLS1s, as well as the other radio-loud AGN classes. Hardening of X-ray spectra during rapid X-ray flares of the radio-loud NLS1 PKS 0558–504 could arise from the transient spectral dominance of synchrotron emission from relativistically boosted jets (Wang et al. 2001), similar to the spectra of radio-loud quasars (e.g., Reeves et al. 1997). Observational evidence for the existence of nonthermal jets and Doppler beaming effect on them are required. If not, the presence of bright radio lobes or a starburst will be needed to explain the radio excess.

Very long baseline interferometry (VLBI) is the most powerful tool available for revealing to such properties by direct imaging. Arcsecond-resolution observations have resolved the structures of only a few NLS1s (Ulvestad et al. 2005; Moran 2000); however, there was insufficient evidence to prove the existence of jets. VLBI images at milli-arcsecond (mas) resolutions had been reported for only three radio-quiet NLS1s: MRK 766, AKN 564 (Lal et al. 2004), and NGC 5506 (Middelberg et al. 2004); pc-scale radio structures were revealed in these NLS1s. VLBI observations on a large number of NLS1s, both radio-quiet and radio-loud objects, are crucial to understand the nature of possible highly energetic jet phenomena in these central engines.

We have started VLBI imaging studies on over a dozen NLS1s, including both radio-quiet and radio-loud objects. It has previously been reported that VLBI observations for the most radio-loud ($R \approx 2000$; Zhou et al. 2003) object, SDSS J094857.3+002225, revealed that Doppler-boosted jets are needed to explain observed high brightness temperatures on its radio emissions (Doi et al. 2006a). In the present paper, we report our VLBI survey of five radio-loud NLS1s at 8.4 GHz. In section 2, we outline the reasons for our selection of NLS1s. In section 3, we describe our observations and data-reduction procedures. In section 4, we present the observational results. In section 5, we discuss the implications of the results. In section 6, we summarize the outcomes of our investigation. Throughout this paper, a flat cosmology is assumed, with $H_0 = 71 \text{ km s}^{-1} \text{ Mpc}^{-1}$, $\Omega_M = 0.27$, and $\Omega_\Lambda = 0.73$ (Spergel et al. 2003).

2. Sample

We selected five targets out of the nine radio-loud NLS1s that were previously identified by Zhou and Wang (2002) from 205 NLS1s listed in “A catalogue of quasars and active nuclei: 10th ed.” (Véron-Cetty & Véron 2001). The reason for the choice is that we could retrieve the National Radio Astronomy Observatory’s (NRAO’s) VLA archival data, obtained at 4.9 or 8.4 GHz with the A-array configuration, which provide radio

Table 1. Radio-loud NLS1 sample for JVN observations.*

Name	z	$S_{1.4\text{GHz}}^{\text{FIRST}}$ (mJy)	$S_{5\text{GHz}}^{\text{VV}}$ (mJy)	$R_{5\text{GHz}}$
(1)	(2)	(3)	(4)	(5)
RXS J08066+7248	0.0980	49.6 [†]	20	85
RXS J16290+4007	0.2720	11.9	22	182
RXS J16333+4718	0.1161	65.0	47	105
RXS J16446+2619	0.1443	90.8	99	200
B3 1702+457	0.0604	118.6	26	11

* (1) source name; (2) redshift; (3) 1.4 GHz flux density from the Faint Images of the Radio Sky at Twenty-centimeters (FIRST; $\sim 5''$ resolution; Becker et al. 1995); (4) 5 GHz flux density (Véron-Cetty & Véron 2001); (5) radio loudness in Zhou & Wang (2002), which were derived from 5 GHz flux density and V-band magnitude listed in Véron-Cetty & Véron (2001) assuming a spectral index of -0.5 .

[†] Flux density at 1.4 GHz from the NRAO VLA Sky Survey (NVSS; $\sim 45''$ resolution; Condon et al. 1998).

positions with sufficient accuracy for processing in a VLBI correlator. Our sample of the five radio-loud NLS1s is listed in table 1.

3. Observations and Data Reduction

3.1. JVN Observations

The five radio-loud NLS1s were observed at 8.4 GHz with the Japanese VLBI Network (JVN), a newly-established VLBI network, with baselines ranging over 50–2560 km, spread across the Japanese islands (K. Fujisawa et al. in preparation; Doi et al. 2006b). This array consists of ten antennas, including four radio telescopes of the VLBI Exploration of Radio Astrometry project (VERA; Kobayashi et al. 2003). The observation dates and telescope participants are listed in table 2. Right-circular polarization was received in two frequency bands, 8400–8416 MHz (IF1) and 8432–8448 MHz (IF2), providing a total bandwidth of 32 MHz. The VSOP-terminal system was used as a digital back-end; digitized data in 2-bit quantization were recorded onto magnetic tapes at a data rate of 128 Mbps. Correlation processing was performed using the Mitaka FX correlator (Shibata et al. 1998) at the National Astronomical Observatory of Japan.

Because the targets in milli-Jansky are too weak for fringe detection with a short integration period, we used a phase-referencing technique that involved fast switching of the antenna’s pointing direction. The switching-cycle period was usually 5 minutes, or ~ 3 minutes at low elevations. For three targets (RXS J08066+7248, RXS J16333+4718, and B3 1702+457), we adopted observation schedules for bigradient phase referencing (BPR; Doi et al. 2006c) using two calibrators: ...-C1-C2-C1-C2-C1-C2-C1-T-C1-T-C1-T-C1-..., where C1, C2, and T represent the primary calibrator, the secondary calibrator, and the desired target, respectively. C1 should be strong enough to be detected in a few minutes. Even if C2 is a fringe-undetectable calibrator in a few minutes, the BPR can make it a fringe-detectable one by

Table 2. JVN observations.*

Date	Antennas [†]	ν (GHz)	Target	$t_{\text{scan}} \times N_{\text{scan}}$ (s)
(1)	(2)	(3)	(4)	(5)
2006Mar17	VMI VIR VIS GIF Ks Ud YMG	8.424	RXS J08066+7248	130×45
2006Mar26	VERA×4 GIF Ks TKB YMG	8.424	RXS J08066+7248	130×6
			RXS J16290+4007	120×22
			RXS J16446+2619	120×16
2006May20	VERA×4 GIF Ks Ud TKB YMG	8.424	RXS J16333+4718	158×15
			B3 1702+457	162×18

* (1) observation date; (2) antenna participant; (3) observing frequency at band center; (4) target name; (5) scan length in second and number of scans.

[†] Station code – Ks: Kashima 34 m of NICT, Ud: Usuda 64 m of JAXA, YMG: Yamaguchi 32 m of NAOJ, TKB: Tsukuba 32 m of GSI, GIF: Gifu 11 m of Gifu University, VMI: VERA Mizusawa 20 m, VIR: VERA Iriki 20 m, VOG: VERA Ogasawara 20 m, and VIS: VERA Ishigaki 20 m of NAOJ.

Table 3. Phase-reference calibrators.*

Target	Calibrators	$\Delta\theta$ (deg)
(1)	(2)	(3)
RXS J08066+7248	J0808+7315 [†]	0.46
	JVAS 0754+7140	1.44
RXS J16290+4007	J1625+4134 [†]	1.56
	J1623+3909	1.50
	NRAO 512	2.23
RXS J16333+4718	J1637+4717 [†]	0.74
	J1628+4734	0.85
RXS J16446+2619	J1642+2523 [†]	1.04
B3 1702+457	J1707+4536 [†]	0.67
	B3 1702+460	0.32

* (1) target's name; (2) calibrator's name; (3) separation angle between target and calibrator.

[†] Primary calibrator as C1 (subsection 3.1).

coherent integration of phase-referenced data for several tens of minutes. The detected C2 will be used as either (1) an alternative focal point, instead of C1, to reduce the separation angle between a target and the calibrator or (2) a tracer to measure undesirable phase-drifts in the sky in order to shift the focus to the nearest point from T on the line of C1–C2 (Doi et al. 2006c). For B3 1702+457, because the three sources were not in alignment, we used C2 as (1). For RXS J16290+4007, we scheduled two secondary calibrators (as “C2” and “C3”) around the target in order to measure two-dimensional phase-gradients in the sky (cf., Fomalont & Kogan 2005). For RXS J16446+2619, no secondary calibrator was used, because we expected to detect this relatively strong target without BPR. See table 3.

3.2. Data Reduction

Data-reduction procedures were performed by following the standard procedures of data inspection, flagging, fringe-fitting, and bandpass calibration using the Astronomical Image

Processing System (AIPS; Greisen 2003) developed at the US National Radio Astronomy Observatory. A standard a priori amplitude calibration was not used, mainly because several JVJN antennas were not equipped with the monitoring system of system noise temperature, T_{sys} . Amplitude-gain parameters relative to each antenna were obtained by self-calibration for a point-like strong source, which was near a target in the sky and scanned every several tens of minutes. A scaling factor of absolute amplitude was obtained from the result of an a priori calibration using the aperture efficiencies and T_{sys} logs of only three antennas (Yamaguchi 32 m, Kashima 34 m, Usuda 64 m) with the T_{sys} monitors. Such a flux calibration appeared to achieve an accuracy level of 10% or less, according to several experiments on the JVJN.

We obtained correction parameters for both the amplitude and the phase by self-calibration of C1 with the AIPS task CALIB using a source structure model, which was established in the Difmap software (Shepherd 1997) using deconvolution and self-calibration algorithms iteratively. The correction parameters were applied to the data of T, C2, and C3. After correcting the positions of the phase-referenced C2 and C3, we derived phase-drift curves from the solutions of self-calibration on both C2 and C3. The amplitude of the phase-drift curves was appropriately scaled-up/down by factors that should be determined from the ratios of the separation angles and the position angles of the target–calibrator pairs (Doi et al. 2006c). For the observations of RX J16333+4719, RX J08066+7248, and RX J16446+2619, the C2–C1 pair is almost parallel to the T–C1 pair in the sky. Therefore, we determined the scaling factors so that $\vec{C}_1\vec{C}_2' = r_{12}\vec{C}_1\vec{C}_2$, where C2' is the nearest point on the C1–C2 line from T and r_{12} is the scaling factor. For the data of RXS J16290+4007 including C2 and C3, we determined two scaling factors so that $\vec{C}_1\vec{T} = r_{12}\vec{C}_1\vec{C}_2 + r_{13}\vec{C}_1\vec{C}_3$. The target and the calibrators in B3 1702+457 observation do not align. Hence, we applied to T the raw solutions of self-calibration on C2, implying that we obtained a closer reference point by replacing C1 with C2.

Imaging and deconvolution of the calibrated data were carried out using Difmap. Frequency averaging was done in

each IF of 16 MHz, resulting in a field of view of $\sim 0''.3$ due to bandpass smearing. We tentatively searched emission components with peak intensities larger than 5σ of the noise on natural-weighting images in the field of view. We detected all five targets. After adjusting the mapping centers to the positions of the emission peaks, we re-imaged them.

Astrometric measurements were made in these images using the JMFIT of AIPS task. In addition, we performed self-calibration on four sources only in phase, and obtained solution parameters for all available antennas with signal-to-noise ratios of more than 3.0. The image dynamic ranges have slightly improved. Self-calibration could not be performed on RXS J08066+7248 because of its weakness. A residual phase-drift in the phase-referenced (i.e., not self-calibrated) data of RXS J08066+7248 can be estimated from those of the secondary calibrator, JVAS 0754+7140, because this type of phase error is mainly dependent on the separation angle of the source pair (Beasley & Conway 1995). The root-mean-square (RMS) of the phase error in the phase-referenced JVAS 0754+7140 was measured, and found to be 39° ; the separation angles of RXS J08066+7248 and JVAS 0754+7140 from J0808+7315 are $0^\circ.46$ and $1^\circ.87$, respectively. Therefore, the phase error in RXS J08066+7248 was estimated to be $9^\circ.6$, causing a coherence loss of only a few percent in amplitude.

4. Results

We detected each of the five radio-loud NLS1s in mas resolutions, as shown in figure 1. These are the first VLBI images for these NLS1s. A single emission component is seen in each image with dynamic ranges of 7.9–75 (table 4). Flux measurements were carried out by elliptical-Gaussian fitting to the source profiles using the JMFIT of AIPS task. The flux densities were 7–150 mJy; the values of the radio loudness, simply derived from the 8.4 GHz JVN flux densities, were still in the radio-loud regime for all of the objects, except for B3 1702+457. The radio powers in the rest frame are listed in table 5.

All sources were unresolved in the JVN beams, resulting in brightness temperatures higher than 2.8×10^7 – 1.1×10^9 K in the rest frame (table 5), which were calculated using

$$T_B = 1.8 \times 10^9 (1+z) \frac{S_\nu}{\nu^2 \phi_{\text{maj}} \phi_{\text{min}}} \quad (1)$$

in K, where z is the redshift, S_ν is the flux density in mJy at frequency ν in GHz, ϕ_{maj} and ϕ_{min} in mas are the fitted full widths at half maximum of the major and minor axes of the source size, respectively (cf., Ulvestad et al. 2005). Because these were unresolved, we adopted one-half the beam sizes, i.e., $\theta/2$ (table 4), as the upper limits to the source sizes, ϕ .

The 8.4 GHz JVN flux densities for the two most radio-loud objects in our sample, RXS J16290+4007 and RXS J16446+2619, were larger than the 1.4 GHz VLA ones (tables 1 and 5). Although the difference between the beam sizes of VLA and JVN causes a resolution effect, we can obtain at least the lower limit of the spectral index, α ($S_\nu \propto \nu^{+\alpha}$). Hence, the two inverted ($\alpha > 0$) spectra must be real, without any regard for possible flux variability.

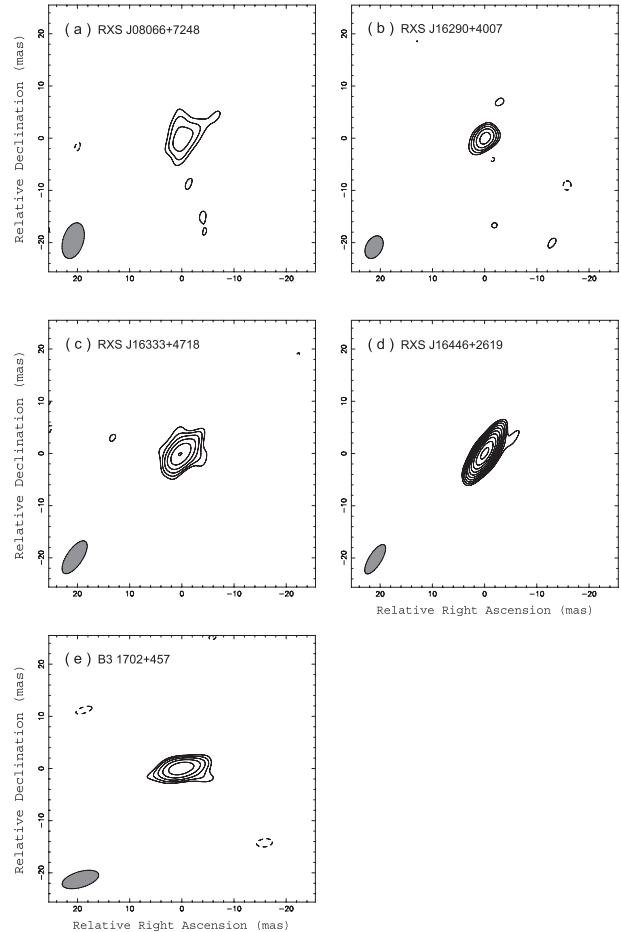


Fig. 1. JVN images of radio-loud NLS1s at 8.4 GHz. The source name is indicated at the upper-left corner in each panel. Data of all sources, except for RXS J08066+7248, were self-calibrated (subsection 3.2). All images were synthesized in natural weighting. Contour levels are separated by factors of $\sqrt{2}$, beginning at 3-times the RMS of the image noise (table 4). Negative and positive contours are shown as dashed and solid curves, respectively. Half-power beam sizes (table 4) are given in the lower left corners.

5. Discussion

We discuss the origin of the detected radio flux densities, and what makes these NLS1s radio-loud, in the present paper. Possible radio emitting sources with relatively high brightness temperatures in active galaxies are (1) an accretion disk, (2) a circumnuclear ionized torus, (3) compact super-nova remnants (SNRs), and (4) AGN jets.

An effective temperature in an accretion disk would be at most 10^7 K, even in the innermost region (within several times the Schwarzschild radius) of a “slim disk,” a theoretical model for super-Eddington accretion (Abramowicz et al. 1988), which may be a possible central engine for NLS1s (e.g., Mineshige et al. 2000; Wang & Netzer 2003). The emissions from such a small region and a relatively low temperature could hardly account for the detected radio fluxes with JVN. The nucleus of the classical Seyfert galaxy, NGC 1068, has a component, S1, that may trace thermal free-free emissions from the ionized region of the innermost (~ 1 pc) molecular

Table 4. Parameters of JVN images.*

Name	σ (mJy beam ⁻¹)	$\theta_{\text{maj}} \times \theta_{\text{min}}$ (mas × mas)	PA (deg)	DR	l (pc mas ⁻¹)
(1)	(2)	(3)	(4)	(5)	(6)
RXS J08066+7248	0.54	3.9 × 7.1	-17	7.7	1.8
RXS J16290+4007	1.82	3.1 × 4.7	-29	15	4.1
RXS J16333+4718	0.93	3.0 × 7.3	-34	16	2.1
RXS J16446+2619	1.94	2.4 × 6.5	-32	75	2.5
B3 1702+457	0.95	3.0 × 7.3	-74	16	1.2

* (1) target's name; (2) RMS of image noise; (3) FWHMs of major and minor axes of synthesized beam; (4) position angle of the beam major axis; (5) image dynamic range, defined as the ratio of peak intensity to RMS of image noise; (6) linear scale in pc corresponding to 1 mas at the distance to the source.

Table 5. Observational results.*

Name	Astrometric position (J2000.0)		$S_{8.4\text{GHz}}^{\text{VLBI}}$ (mJy)	$I_{8.4\text{GHz}}^{\text{VLBI}}$ (mJy beam ⁻¹)	$P_{8.4\text{GHz}}$ (W Hz ⁻¹)	T_{B} (K)
(1)	RA	Dec	(4)	(5)	(6)	(7)
RXS J08066+7248	08 06 38.95744	72 48 20.4042	6.9 ± 1.4	4.2 ± 0.7	23.2	> 10 ^{7.4}
RXS J16290+4007	16 29 01.31060	40 07 59.9061	26.3 ± 4.0	27.2 ± 3.3	24.6	> 10 ^{8.4}
RXS J16333+4718	16 33 23.58079	47 18 58.9298	21.2 ± 2.9	15.0 ± 1.8	23.8	> 10 ^{8.0}
RXS J16446+2619	16 44 42.53399	26 19 13.2257	150.6 ± 15.4	145.5 ± 14.7	24.8	> 10 ^{9.0}
B3 1702+457	17 03 30.38302	45 40 47.1679	18.5 ± 2.6	15.1 ± 1.8	23.2	> 10 ^{8.0}

(1) target's name; (2)–(3) astrometric position, measured relative to C1, by our phase-referenced VLBI observation. The position uncertainty was 1 mas or less, which was dominated by absolute-position uncertainties of C1 as an ICRF source (Ma et al. 1998; Fey et al. 2004); (4) flux density. The error was determined as the root-sum-square of the flux calibration error (10%; subsection 3.2) and the Gaussian-fitting error (section 4); (5) peak intensity; (6) radio power at a rest frequency of 8.4 GHz, in which K -correction was applied assuming a two-point spectral index derived from VLA at 1.4 GHz (table 1) and JVN flux density at 8.4 GHz; (7) brightness temperature at the rest frame [equation (1)].

torus (Gallimore et al. 2004). However, this is an exceptional example, and its brightness temperature was at most $\sim 10^6$ K, far inferior when compared with the detected radio-loud NLS1s.

The measured brightness temperatures, $T_{\text{B}} > 2.8 \times 10^7 - 1.1 \times 10^9$ K (table 5), were quite high, which is evidence for the existence of a nonthermal process. Many VLBI detections have been reported for very young, compact SNRs, for example, SN 1993J (Bietenholz et al. 2001). However, even the most luminous radio SNR, SN 1988Z ($z \approx 0.022$), generated radio power at 8.4 GHz of $\sim 10^{21.3}$ W Hz⁻¹ at the maximum in its light curve (van Dyk et al. 1993). The sources detected with JVN clearly exceed this limit, excluding a compact SNR origin. Although the radio powers taken from a sample of the most radio-luminous starbursts are $\sim 10^{22.3} - 10^{23.4}$ W Hz⁻¹ (Smith et al. 1998), these brightness temperatures were derived to be $\lesssim 10^5$ K, much less than those of the detected radio-loud NLS1s. Thus, a stellar origin should be ruled out.

Previously, based on a sensitivity of $\sim 10^6 - 10^8$ K, VLBI imaging has been used to prove that radio emissions associated with AGNs are powered by a nonthermal process related to the activity of a central engine, not only for strong radio AGN classes, but also for weak radio AGN classes, such as Seyfert galaxies (e.g., Preuss & Fosbury 1983; Neff &

de Bruyn 1983) and radio-quiet quasars (e.g., Blundell & Beasley 1998; Ulvestad et al. 2005). The radio emissions detected from our NLS1 sample are also likely to be related to the activity of central engines. Nonthermal jets are presumably associated with them, although the JVN images did not resolve any structures. SDSS J094857.3+002225, the most radio-loud NLS1, has been resolved with VLBI into multiple radio components with very high brightness temperatures, requiring Doppler boosting (Doi et al. 2006a), indicating highly relativistic jets. Possible jet structures have also been found with VLBI in NGC 5506 (Middelberg et al. 2004), a radio-quiet NLS1 candidate (Nagar et al. 2002). In the limited dynamic ranges, the JVN images have presumably shown an unresolved core as the base of jets, or one of the compact hot-spots in radio lobes in these radio-loud NLS1s.

We now discuss the relationship between the radio loudness and the radio spectral index. We made a plot of radio loudness vs. radio power using (a) the nine radio-loud NLS1s listed in Zhou and Wang (2002), including the five NLS1s observed with JVN (see, section 2), and (b) the most radio-loud narrow-line quasar SDSS J094857.3+002225 ($R \approx 2000$; Zhou et al. 2003), as shown in figure 2. RXS J00449+1921, one of the sample in Zhou & Wang (2002), was excluded from the plot because recent observations have found it

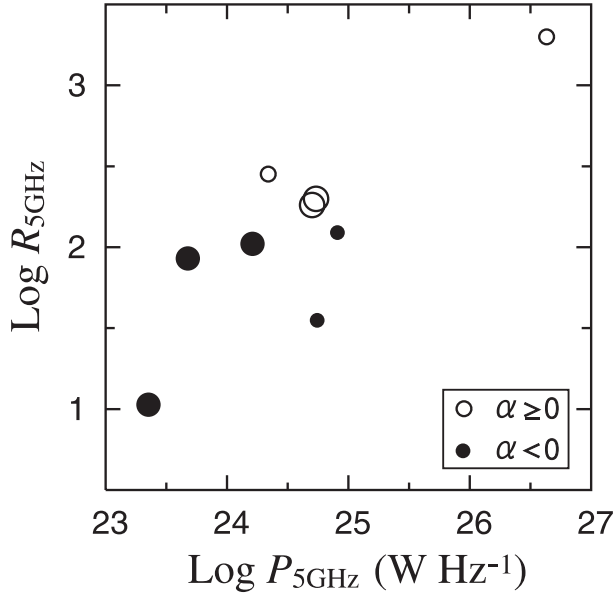


Fig. 2. Radio loudness vs. 5 GHz radio power for the sample of radio-loud NLS1s from Zhou and Wang (2002) and Doi et al. (2006a). The radio data were taken mainly from Véron-Cetty and Véron (2001); see section 4 for details. The filled and open circles represent objects with a steep spectrum and an inverted spectrum, respectively ($S_\nu \propto \nu^{+\alpha}$). Five large plots represent objects observed with JVN in the present study.

to be radio-quiet (Maccarone et al. 2005). The total flux densities at 1.4–5 GHz were taken from Véron-Cetty and Véron (2001) for these NLS1s, except for HE 0132–4313 at 4.85–8.4 GHz (Grupe et al. 2000), PKS 0558–504 at 2.7–4.85 GHz (Wright & Otrupcek 1990; Wright et al. 1994), and SDSS J094857.3+002225 at 1.43–4.86 GHz (Doi et al. 2006a). We discovered that the four inverted spectrum sources are the four most radio-loud objects: SDSS J094857.3+002225 with $R \approx 2000$, 2E 1640+5345 with $R = 282$, RXS J16446+2619 with $R = 200$, and RXS J16290+4007 with $R = 182$. This suggests that there could be some connection between a strong low-frequency absorption and the high values of radio loudness. We discuss two possibilities to cause the combination of the high radio loudness and the strong absorption. (1) One possibility is the Doppler beaming effect on jets. The radio flux density from jets could have been boosted by a factor of $\delta^{3-\alpha}$ where Doppler factor $\delta \equiv \sqrt{1-\beta^2}/(1-\beta \cos \phi)$, $\beta \equiv v/c$ (v is the source speed), and ϕ is the angle between the direction of the source velocity and our line of sight, although the optical emission from the accretion disk is not affected; a higher radio loudness could be achieved. The peak frequency of a self-absorbed synchrotron spectrum could be enhanced by a factor of δ . The frequency range where an inverted spectrum could be seen would extend to our observing frequency. Doppler beaming in an NLS1 has already been established by variability (Zhou et al. 2003) and VLBI studies (Doi et al. 2006a) for SDSS J094857.3+002225, the most radio-loud object in figure 2. (2) Another possibility is a very compact radio lobe. Giga-hertz peaked spectrum objects (GPSs; O’Dea 1998 for a review) are strong, compact radio sources, and are thought

to be in a very early stage ($< 10^3$ yr) in the evolution of radio galaxies. The radio lobes of GPSs are probably self-absorbed due to high brightness, and their spectral evolution throughout the evolution of a radio galaxy has been suggested (e.g., Snellen et al. 2000). According to the evolution framework, radio lobes become more luminous and less absorbed with age. However, although we used a limited number of radio-loud NLS1s, we cannot find any evidence of such an expected tendency in figure 2: inverted (i.e., strongly absorbed) spectra are rather seen at a high radio power regime. It is less likely that radio-loud NLS1s are a kind of GPSs. Therefore, we suggest the possibility that Doppler boosting has affected the radio loudness of these NLS1s showing inverted spectra.

We also have radio-loud NLS1s with steep ($\alpha < 0$) spectra. At least our VLBI detections have revealed the existence of components with high brightness temperatures in the three steep spectrum radio-loud NLS1s, as well as the two inverted spectrum ones. In the case of $\alpha = -0.6$, more than about half of the 1.4 GHz VLA flux densities (table 1) have been retrieved with JVN at 8.4 GHz, implying that a compact nonthermal component made a major contribution toward the total radio fluxes. However, we have only a few suggestions about the reason why they are radio-loud. There may be the following possibilities. (1) Doppler beaming may exist, but mildly affected: there would be an insufficient boosting on frequency, but a sufficient boosting on radio flux to the observables, due to only δ -times boosting on frequency, but $\delta^{3-\alpha}$ -times boosting on flux density. (2) These NLS1s may have significant jet structures that can provide a radio power sufficient to being radio-loud, but cannot be resolved at a spatial resolution of JVN, $\sim 3 \text{ mas} \times 7 \text{ mas}$. Under the condition of equipartition between synchrotron electrons and magnetic fields, a diameter of about 0.4 mas or more would be needed for a component size in these NLS1s, so that a jet can be optically-thin (i.e., steep spectrum) at frequencies higher than 1.4 GHz. Even if radio lobes with a size of 1 mas or less possibly resided in these NLS1s, they could not be resolved with JVN beams. We cannot rule out either of the possibilities based only on the present study.

We carried out another VLBI observation for the same sample at 1.7 GHz with the US Very Long Baseline Array (VLBA); the results will be reported in a future paper. We expect that the radio properties of the radio-loud NLS1s will be revealed in more detail, because optically thin, extended synchrotron emissions would be detected more easily at such a low frequency.

6. Summary

We observed five radio-loud NLS1s at 8.4 GHz with the Japanese VLBI Network (JVN) using a phase-referencing technique. All of the targets were detected and unresolved in mas resolutions, i.e., with brightness temperatures higher than 10^7 – 10^9 K. VLBI-detected flux densities kept four out of the five sources still radio-loud. Radio powers mainly originate in the nonthermal processes of AGN activity in the central engines, rather than starbursts. We argued about the properties of nonthermal jets in these NLS1s. The two most radio-loud objects in our sample, RXS J16290+4007 and

RXS J16446+2619, showed inverted spectra between the VLA flux densities at 1.4 GHz and JVN ones at 8.4 GHz. With nine radio-loud NLS1s, we also found that the four most radio-loud objects exclusively have inverted spectra. We suggest there is a possibility that the radio emissions of these NLS1s are enhanced by Doppler beaming, which can change both the radio loudness and the peak frequency of the synchrotron self-absorption spectra.

The JVN project is led by the National Astronomical Observatory of Japan (NAOJ), which is a branch of the National Institutes of Natural Sciences (NINS), Hokkaido

University, Gifu University, Yamaguchi University, and Kagoshima University, in cooperation with the Geographical Survey Institute (GSI), the Japan Aerospace Exploration Agency (JAXA), and the National Institute of Information and Communications Technology (NICT). We have made use of NASA's Astrophysics Data System Abstract Service, the NASA/IPAC Extragalactic Database (NED), which is operated by the Jet Propulsion Laboratory; it also has made use of Ned Wright's on-line cosmology calculator. The US National Radio Astronomy Observatory is a facility of the National Science Foundation operated under cooperative agreement by Associated Universities, Inc.

References

- Abramowicz, M. A., Czerny, B., Lasota, J. P., & Szuszkiewicz, E. 1988, *ApJ*, 332, 646
- Beasley, A. J., & Conway, J. E. 1995, in *ASP Conf. Ser.* 82: Very Long Baseline Interferometry and the VLBA, 82, 328
- Becker, R. H., White, R. L., & Helfand, D. J. 1995, *ApJ*, 450, 559
- Bietenholz, M. F., Bartel, N., & Rupen, M. P. 2001, *ApJ*, 557, 770
- Blundell, K. M., & Beasley, A. J. 1998, *MNRAS*, 299, 165
- Boroson, T. A. 2002, *ApJ*, 565, 78
- Condon, J. J., Cotton, W. D., Greisen, E. W., Yin, Q. F., Perley, R. A., Taylor, G. B., & Broderick, J. J. 1998, *AJ*, 115, 1693
- Doi, A., et al. 2006b, in *Proc. 8th European VLBI Netw. Symp.*, ed. Baan Willem et al., 71
- Doi, A., et al. 2006c, *PASJ*, 58, 777
- Doi, A., Nagai, H., Asada, K., Kameno, S., Wajima, K., & Inoue, M. 2006a, *PASJ*, 58, 829
- Fey, A. L., et al. 2004, *AJ*, 127, 3587
- Fomalont, E. B., & Kogan, L. R. 2005, Phase referencing with more than one calibrator using ATMCA, AIPS Memo No. 111
- Gallimore, J. F., Baum, S. A., & O'Dea, C. P. 2004, *ApJ*, 613, 794
- Greene, J. E., Ho, L. C., & Ulvestad, J. S. 2006, *ApJ*, 636, 56
- Greisen, E. W. 2003, in *Information Handling in Astronomy — Historical Vistas*, ed. A. Heck (Dordrecht: Kluwer), 109
- Grupe, D., Leighly, K. M., Thomas, H.-C., & Laurent-Muehleisen, S. A. 2000, *A&A*, 356, 11
- Grupe, D., & Mathur, S. 2004, *ApJ*, 606, L41
- Kellermann, K. I., Sramek, R. A., Schmidt, M., Green, R. F., & Shaffer, D. B. 1994, *AJ*, 108, 1163
- Kobayashi, H., et al. 2003, *ASP Conf. Ser.*, 306, 367
- Komossa, S., Voges, W., Adorf, H.-M., Xu, D., Mathur, S., & Anderson, S. F. 2006b, *ApJ*, 639, 710
- Komossa, S., Voges, W., Xu, D., Mathur, S., Adorf, H.-M., Lemson, G., Duschl, W. J., & Grupe, D. 2006a, *AJ*, 132, 531
- Lal, D. V., Shastri, P., & Gabuzda, D. C. 2004, *A&A*, 425, 99
- Ma, C., et al. 1998, *AJ*, 116, 516
- Maccarone, T. J., Miller-Jones, J. C. A., Fender, R. P., & Pooley, G. G. 2005, *A&A*, 433, 531
- McClintock, J. E., & Remillard, R. A. 2003, (*astro-ph/0306213*)
- Middelberg, E., et al. 2004, *A&A*, 417, 925
- Mineshige, S., Kawaguchi, T., Takeuchi, M., & Hayashida, K. 2000, *PASJ*, 52, 499
- Moran, E. C. 2000, *New Astron. Rev.*, 44, 527
- Nagar, N. M., Oliva, E., Marconi, A., & Maiolino, R. 2002, *A&A*, 391, L21
- Neff, S. G., & de Bruyn, A. G. 1983, *A&A*, 128, 318
- O'Dea, C. P. 1998, *PASP*, 110, 493
- Osterbrock, D. E., & Pogge, R. W. 1985, *ApJ*, 297, 166
- Peterson, B. M., et al. 2000, *ApJ*, 542, 161
- Pogge, R. W. 2000, *New Astron. Rev.*, 44, 381
- Pounds, K. A., Done, C., & Osborne, J. P. 1995, *MNRAS*, 277, L5
- Preuss, E., & Fosbury, R. A. E. 1983, *MNRAS*, 204, 783
- Reeves, J. N., Turner, M. J. L., Ohashi, T., & Kii, T. 1997, *MNRAS*, 292, 468
- Shepherd, M. C. 1997, in *ASP Conf. Ser.* 125, *Astronomical Data Analysis Software and Systems VI* (San Francisco: ASP), 77
- Shibata, K. M., Kameno, S., Inoue, M., & Kobayashi, H. 1998, in *ASP Conf. Ser.* 144, *IAU Colloq. 164: Radio Emission from Galactic and Extragalactic Compact Sources* (San Francisco: ASP), 413
- Siebert, J., Leighly, K. M., Laurent-Muehleisen, S. A., Brinkmann, W., Boller, T., & Matsuoka, M. 1999, *A&A*, 348, 678
- Smith, D. A., Herter, T., & Haynes, M. P. 1998, *ApJ*, 494, 150
- Snellen, I. A. G., Schilizzi, R. T., Miley, G. K., de Bruyn, A. G., Bremer, M. N., & Röttgering, H. J. A. 2000, *MNRAS*, 319, 445
- Spergel, D. N., et al. 2003, *ApJS*, 148, 175
- Stoche, J. T., Morris, S. L., Weymann, R. J., & Foltz, C. B. 1992, *ApJ*, 396, 487
- Ulvestad, J. S., Antonucci, R. R. J., & Barvainis, R. 2005, *ApJ*, 621, 123
- Ulvestad, J. S., Antonucci, R. R. J., & Goodrich, R. W. 1995, *AJ*, 109, 81
- van Dyk, S. D., Weiler, K. W., Sramek, R. A., & Panagia, N. 1993, *ApJ*, 419, L69
- Véron-Cetty, M.-P., & Véron, P. 2001, *A&A*, 374, 92
- Visnovsky, K. L., Impey, C. D., Foltz, C. B., Hewett, P. C., Weymann, R. J., & Morris, S. L. 1992, *ApJ*, 391, 560
- Wang, J.-M., & Netzer, H. 2003, *A&A*, 398, 927
- Wang, T. G., Matsuoka, M., Kubo, H., Mihara, T., & Negoro, H. 2001, *ApJ*, 554, 233
- Whalen, D. J., Laurent-Muehleisen, S. A., Moran, E. C., & Becker, R. H. 2006, *AJ*, 131, 1948
- Wright, A., & Otrupcek, R. 1990, *Parkes Radio Sources Catalogue*
- Wright, A. E., Griffith, M. R., Burke, B. F., & Ekers, R. D. 1994, *ApJS*, 91, 111
- Zhou, H.-Y., & Wang, T.-G. 2002, *Chinese J. Astron. Astrophys.*, 2, 501
- Zhou, H.-Y., Wang, T.-G., Dong, X.-B., Zhou, Y.-Y., & Li, C. 2003, *ApJ*, 584, 147